FED-Vol. 116

CAVITATION '91

presented at
THE FIRST ASME•JSME FLUIDS ENGINEERING CONFERENCE
PORTLAND, OREGON
JUNE 23–27, 1991

co-sponsored by
THE FLUIDS ENGINEERING DIVISION, ASME
THE FLUIDS ENGINEERING DIVISION, JSME

edited by
H. KATO
UNIVERSITY OF TOKYO

O. FURUYA
OF TECHNOLOGIES, INC.

THE AMERICAN SOCIETY OF MECHANICAL ENGINEERS
United Engineering Center 345 East 47th Street New York, N.Y. 10017

FED-Vol. 116, Cavitation '91
ASME 1991

ANALYTICAL APPROACHES TO MODELING TRANSIENT VAPOROUS CAVITATION IN MULTI-PIPE FLUID SYSTEMS

T. W. Walters
Thermodynamics Group
General Dynamics Space Systems Division
San Diego, California

ABSTRACT

An extension of the Vaporous Cavitation Model method for modeling vapor cavity formation during liquid column separation in transient flows is made to eight common fluid system connecting elements. A comparison to experimental data for three of the elements is made to recent data for a nonstraight pipe. Reasonable agreement with the data is shown, although very large vapor cavities occur in the system.

NOMENCLATURE

A	pipe cross-sectional area
A_G	valve flow area
a	wavespeed
B	pipe impedance, $a/(gA)$
C_D	discharge coefficient
C_V	valve flow coefficient, $Q_o^2\tau^2/(2\Delta H_o)$
D	diameter
F	force
f	friction factor
g	acceleration due to gravity
H	piezometric head
H_A	absolute head
H_{BAR}	barometric pressure head (absolute)
H_{check}	differential head required to open a closed check valve
H_E	head downstream of valve flowing out of system (relative)
H_V	vapor pressure head (absolute)
L	length
Q	volumetric flowrate
Q_U	volumetric flowrate on upstream side of vapor cavity
R	pipe resistance, $f\Delta x/(2gDA^2)$
R_{check}	flow resistance through check valve
t	time
V	volume
v	velocity
x	distance
z	elevation above arbitrary datum
ρ	liquid density
τ	valve open ratio, $C_DA_G/(C_DA_G)_o$

Subscripts

CAV	cavity
i	position
NS	last section of a pipe
o	reference value
P	current time step

INTRODUCTION

The formation of vapor cavities in piping systems experiencing column separation during liquid transient flow is of engineering interest because of the very high transient pressures that can occur when the vapor cavities collapse. Several approaches have been proposed for modeling vaporous cavitation in single-pipe fluid systems. One approach for modeling this phenomenon is the Vaporous Cavitation Model (VCM). The VCM method for a single-pipe system is described by Streeter (1972) and amplified by Wylie and Streeter (1983). In order to model vaporous cavitation in a complex multi-pipe system, analytical expressions are required for the fluid connecting elements that join the pipes together. Although the VCM method has been used for many years, it is difficult to find descriptions in the open literature of how the VCM method is applied to common fluid system connecting elements. This paper describes how the VCM method was applied at General Dynamics Space Systems Division.

SINGLE-PIPE VCM METHOD

The starting point for any investigation of column separation begins with the basic equations of waterhammer (Wylie, 1984a). These equations consist of two partial differential equations that are derived from the continuity and one-dimensional momentum equation. When applied to a stiff liquid-filled pipe, the equations are expressed:

$$\frac{\partial H}{\partial t} + \frac{a^2}{g}\frac{\partial v}{\partial x} = 0$$

$$g\frac{\partial H}{\partial x} + \frac{\partial v}{\partial t} + \frac{f}{2D} v|v| = 0$$

The method of characteristics is then used to reduce the equations to a series of four ordinary differential equations (Streeter, 1972, and Wylie and Streeter, 1983). Finite difference techniques reduce the equations further to algebraic form, which allows solution by digital computer. When written in difference equation form, two unknowns are left to be determined after selection of the distance and time computation steps. The two unknowns, piezometric head, $H_{P,i}$, and volumetric flowrate, $Q_{P,i}$, are determined for pipe section i at time P from the following equations (Wylie and Streeter, 1983):

$$H_{P,i} = C_P - B\,Q_{P,i} \tag{1}$$

$$H_{P,i} = C_M + B\,Q_{P,i} \tag{2}$$

where C_P and C_M are known constants for the current time step,

$$C_P = H_{i-1} + B\,Q_{i-1} - R\,Q_{i-1}|Q_{i-1}| \tag{3}$$

$$C_M = H_{i+1} - B\,Q_{i+1} + R\,Q_{i+1}|Q_{i+1}| \tag{4}$$

and $R = f\Delta x/(2gDA^2)$ while $B = a/(gA)$. These equations are only valid along the characteristic lines, given by $\Delta t = \pm \Delta x/a$. This approach is often referred to as the method of specified time intervals.

Vapor cavities can form in the pipe when the transient fluid pressure approaches the local vapor pressure. The VCM method assumes that the vapor formation process is a discrete event, occurring at a particular vapor pressure. The vapor pressure of the liquid is assumed to be constant throughout the system. Thus, when the solution for $H_{P,i}$ results in a pressure below the vapor pressure of the liquid, the VCM method assumes that a vapor cavity will form in the pipe. This situation is depicted in detail in Figure 1, adopted from Wylie and Streeter (1983). When a vapor cavity forms, the pressure then becomes a known parameter, being just the vapor pressure of the liquid. However, the formation of a cavity means that the flow into the computing section no longer balances. Thus, in view of Figure 1 and Eqs. (1) and (2),

$$H_{P,i} = H_v + z_i - H_{BAR} \tag{5}$$

$$Q_{PU,i} = \frac{(C_P - H_{P,i})}{B} \tag{6}$$

$$Q_{P,i} = \frac{(H_{P,i} - C_M)}{B} \tag{7}$$

where $Q_{P,i}$ and $Q_{PU,i}$ are the unbalanced flowrates at section i (Figure 1), and H_V is the absolute vapor pressure head. Eq. (4) also becomes

$$C_M = H_{i+1} - B\,Q_{U_{i+1}} + R\,Q_{U_{i+1}}|Q_{U_{i+1}}| \tag{8}$$

Eq. (3) remains unchanged, although $Q_{P,i}$ now represents the flowrate on the downstream side of the cavity (Figure 1). The size of the vapor cavity is determined by integrating the entering and exiting flow over the time step (Streeter, 1972, and Wylie and Streeter, 1983) which gives

$$V_{CAV,P,i} = V_{CAV,i} + (Q_{P,i} + Q_i - Q_{PU,i} - Q_{U,i})\,\Delta t/2$$

where $V_{CAV,i}$ is the cavity size at the previous time step. When $V_{CAV,P,i}$ becomes negative, then the cavity disappears and the pressure is allowed to rise above the vapor pressure, and the solution is again obtained from Eqs. (1) and (2). When no cavities are present, then $Q_P = Q_{PU}$ because the flows must balance.

The VCM method assumes that the vapor is concentrated in discrete cavities in the pipe and that the cavities do not move during the simulation. Further, it is well known that the presence of large vapor cavities will reduce the wavespeed in the system. Thus, the cavities are assumed to be small when compared to the size of the computing section so that a constant wavespeed can be assumed.

VCM CONNECTING ELEMENTS

The solution of a piping network requires analytical expressions to describe the fluid elements that connect the pipes. Eight common connecting elements will be described: branches, valves in a line, check valves in a line, valves at system exit, dead-end pipes, specified flowrate boundary, reservoir (specified head boundary), and short pipes with lumped inertia. The standard methodology for each element when above vapor pressure will be briefly reviewed to provide the context for the cavi-

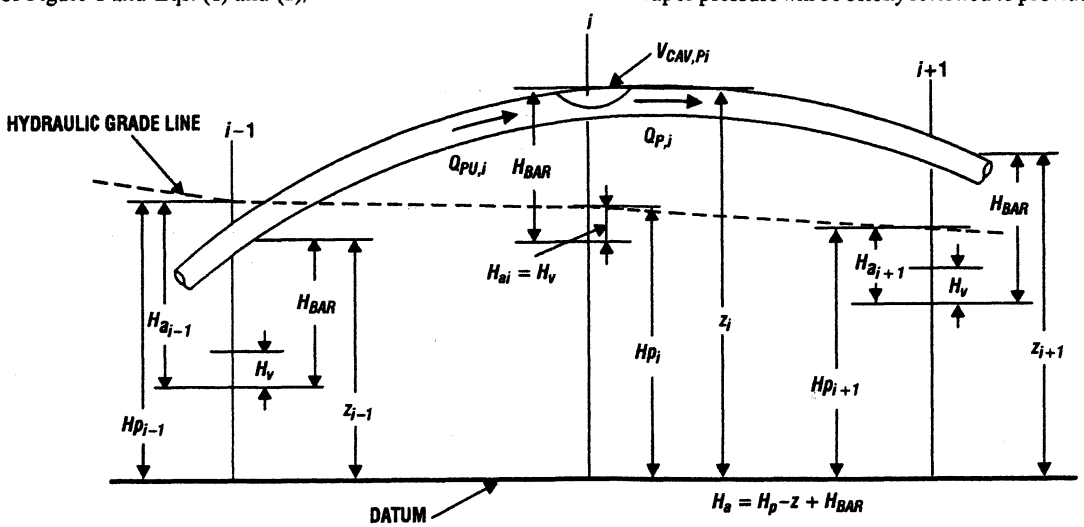

Figure 1. Definition of terms for modeling column separation.

tation methodology. The standard methodology is described in detail by Wylie and Streeter (1983) and Streeter (1972).

Branch Connector

A branch connector models a connection where multiple pipes branch together to join or split the flow. For discussion purposes, a branch with four pipes will be addressed, with two pipes flowing into the branch and two flowing out. Figure 2 depicts this situation. At a branch, mass conservation requires that

$$\Sigma Q_P = 0 \tag{9}$$

and the head at the branch is identical for all pipes. That is,

$$H_P = H_{P\,1,NS} = H_{P\,2,NS} = H_{P\,3,1} = H_{P\,4,1}$$

where the second subscript is the pipe number and the third subscript is the section of that pipe (the subscript "NS" denotes the end section of a pipe). The flowrates for the four pipes are determined from Eqs. (1, 2):

$$Q_{P\,1,NS} = \frac{(-H_P + C_{P1})}{B_1} \tag{10}$$

$$Q_{P\,2,NS} = \frac{(-H_P + C_{P2})}{B_2} \tag{11}$$

$$Q_{P\,3,1} = \frac{(H_P - C_{M3})}{B_3} \tag{12}$$

$$Q_{P\,4,1} = \frac{(H_P - C_{M4})}{B_4} \tag{13}$$

From Eq. (9)

$$\sum Q_P = 0 = -H_P \sum \frac{1}{B} + \sum \frac{C_P}{B} + \sum \frac{C_M}{B}$$

Solving for H_P yields:

$$H_P = \frac{\left(\sum \frac{C_P}{B} + \sum \frac{C_M}{B}\right)}{\sum \frac{1}{B}}$$

When the pressure in the branch drops to the vapor pressure, the approach is similar to the single-pipe method. The heads for all pipes are equal,

$$H_P = H_{P\,1,NS} = H_{P\,2,NS} = H_{P\,3,1} = H_{P\,4,1} = H_V + z_i - H_{BAR}$$

but the flowrates no longer sum to zero because of the forming vapor cavity in the branch. With multiple pipes entering the branch, the Q_{PU} terms are not required to keep track of the flows on different sides of the cavity. The flowrates for each of the pipes are determined from Eqs. (10–13).

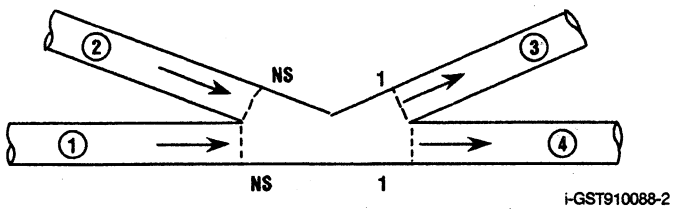

Figure 2. Schematic for branch connector.

Because the branch is common to all pipes, then all pipes contribute to the vapor cavity growth:

$$V_{CAV,P} = V_{CAV} + (Q_{P\,1,NS} + Q_{1,NS} + Q_{P\,2,NS} + Q_{2,NS} - Q_{P\,3,1} - Q_{3,1} - Q_{P\,4,1} - Q_{4,1})\ \Delta t/2$$

$$V_{CAV,P} = V_{CAV,P\,1,NS} = V_{CAV,P\,2,NS} = V_{CAV,P\,3,1} = V_{CAV,P\,4,1}$$

When $V_{CAV,P}$ becomes negative, the cavity collapses and the pressure is again allowed to rise above vapor pressure.

Valve-in-line

The flow through a valve under steady flow conditions is given by

$$Q_o = (C_D A_G)_o \sqrt{2\ g\ \Delta H_o} \tag{14}$$

where Q_o is the steady state flowrate, $(C_D A_G)_o$ is the steady state effective flow area, and ΔH_o is the steady state head loss across the valve. In general,

$$Q_P = C_D A_G \sqrt{2\ g\ \Delta H} \tag{15}$$

Defining $\tau = C_D A_G / (C_D A_G)_o$ and combining Eqs. (14) and (15) yields

$$Q_P = Q_o\ \tau \sqrt{\frac{\Delta H}{\Delta H_o}} \tag{16}$$

Referring to Figure 3, Eq. (16) can be written for forward flows

$$Q_{P\,1,NS} = Q_{P\,2,1} = \frac{Q_o\ \tau}{\sqrt{\Delta H_o}} \sqrt{H_{P\,1,NS} - H_{P\,2,1}} \tag{17}$$

Substituting Eqs. (1) and (2) into Eq. (17) results in a quadratic equation for the flowrate through the valve. The solution of this equation can be shown to be

$$Q_{P\,1,NS} = -C_V(B_1 + B_2) + \sqrt{C_V^2(B_1 + B_2)^2 + 2C_V(C_{P_1} - C_{M_2})}$$

where $C_V = Q_o^2 \tau^2 / (2\Delta H_o)$. For backward flow through the valve it can be shown

$$Q_{P\,1,NS} = C_V(B_1 + B_2) - \sqrt{C_V^2(B_1 + B_2)^2 - 2C_V(C_{P_1} - C_{M_2})}$$

When the pressure at a valve reaches vapor pressure, two situations must be addressed for each flow direction: only one side at vapor pressure and both sides at vapor pressure. For forward flows with the downstream side at vapor pressure, the downstream head, $H_{P\,2,1}$, is given by Eq. (5). $Q_{P\,2,1}$ is given by Eq. (7) and the flowrate through the valve is determined by inserting Eq. (1) into Eq. (17), for which the solution is:

$$Q_{P\,1,NS} = Q_{PU\,1,NS} = Q_{PU\,2,1}$$

$$= -C_v B_1 + \sqrt{C_v^2 B_1^2 - 2C_v(C_{P_1} - H_{P2,1})}$$

$H_{P\,1,NS}$ is then found from Eq. (1). In this case, a vapor cavity forms at the downstream side of the valve, but not on the upstream side.

When both sides of the valve reach vapor pressure, then both $H_{P\,1,NS}$ and $H_{P\,2,1}$ are given by Eq. (5). Since $H_{P\,1,NS} = H_{P\,2,1}$, no fluid can flow through the valve:

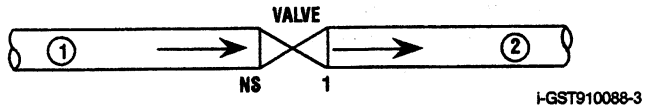

Figure 3. Schematic for valve-in-line connector.

$$V_{CAV,P\,2,1} = V_{CAV\,2,1} + \left(Q_{P\,2,1} + Q_{2,1} - Q_{PU\,2,1} - Q_{U\,2,1}\right)\Delta t/2$$
$$V_{CAV,P\,1,NS} = 0 \qquad (18)$$
$$Q_{P\,1,NS} = Q_{PU\,2,1} = 0$$

$Q_{PU\,1,NS}$ and $Q_{P\,2,1}$ are determined from Eqs. (6) and (7). Vapor forms on both sides of the valve, and the cavity sizes are:

$$V_{CAV,P\,1,NS} = V_{CAV\,1,NS} + \left(Q_{1,NS} - Q_{PU\,1,NS} - Q_{U\,1,NS}\right)\Delta t/2 \qquad (19)$$

$$V_{CAV,P\,2,1} = V_{CAV\,2,1} + \left(Q_{P\,2,1} + Q_{2,1} - Q_{U\,2,1}\right)\Delta t/2 \qquad (20)$$

When the flow through the valve is backwards, the situation is similar to forward flow. For backward flow with one side at vapor pressure it can be shown:

$$Q_{P\,1,NS} = Q_{PU\,2,1} = Q_{P\,2,1}$$
$$= C_v B_2 - \sqrt{C_v^2 B_2^2 + 2C_v\left(C_{M_2} - H_{P\,1,NS}\right)}$$

where $H_{P\,1,NS}$ is determined from Eq. (5). $Q_{PU\,1,NS}$ is determined from Eq. (6) and the vapor cavity forms on the pipe 1 side:

$$V_{CAV,P\,1,NS} = V_{CAV\,1,NS} + \left(Q_{P\,1,NS} + Q_{1,NS} - Q_{PU\,1,NS} - Q_{U\,1,NS}\right)\Delta t \qquad (21)$$
$$V_{CAV,P\,2,1} = 0$$

All other parameters are determined similarly to forward flow.

Check Valve-in-line

When a check valve is open, the head loss through the valve is expressed

$$H_{P\,1,NS} - H_{P\,2,1} = R_{check}\, Q_{P\,1,NS} \left| Q_{P\,1,NS} \right| \qquad (22)$$

where R_{check} is the resistance of the check valve. By continuity, $Q_{P\,1,NS} = Q_{P\,2,1}$. Combining Eq. (22) with Eqs. (1) and (2) and solving the quadratic for $Q_{P\,2,1}$ yields

$$Q_{P\,2,1} = -B_B + \sqrt{B_B^2 + C_C}$$
$$B_B = \frac{B_1 + B_2}{2\,R_{check}} \qquad (23)$$
$$C_C = \frac{C_{P_1} - C_{M_2}}{R_{check}}$$

When $Q_{P\,2,1}$ becomes negative, then the check valve closes and

$$Q_{P\,1,NS} = Q_{P\,2,1} = 0$$
$$H_{P\,1,NS} = C_{P_1}$$
$$H_{P\,2,1} = C_{M_2}$$

When $H_{P\,1,NS} - H_{P\,2,1} > H_{check}$, the valve will reopen and conditions are calculated as described previously.

Vapor cavities can form on the downstream side of the valve when the valve is open, and on both sides of the valve when it is closed. When the valve is open and the downstream side drops to vapor pressure then the downstream head, $H_{P\,2,1}$, is known from Eq. (5) and

$$Q_{P\,2,1} = \frac{H_{P\,2,1} - C_{M_2}}{B_2}$$
$$Q_{PU\,1,NS} = Q_{P\,1,NS} = Q_{PU\,2,1}$$

The flowrate, $Q_{P\,1,NS}$, is expressed by Eq. (23), with the following changes:

$$B_B' = \frac{B_1}{2\,R_{check}}$$
$$C_C' = \frac{C_{P_1} - H_{P\,2,1}}{R_{check}}$$

The vapor cavity size is found from Eq. (18).

When the valve is closed, either or both sides can drop to vapor pressure. When both sides of the check valve reach vapor pressure, then both $H_{P\,1,NS}$ and $H_{P\,2,1}$ are given by Eq. (5), and

$$Q_{P\,1,NS} = Q_{PU\,2,1} = 0$$
$$Q_{PU\,1,NS} = \frac{\left(C_{P_1} - H_{P\,1,NS}\right)}{B_1}$$
$$Q_{P\,2,1} = \frac{\left(H_{P\,2,1} - C_{M_2}\right)}{B_2}$$

The vapor cavity sizes are determined from Eqs. (19) and (20). When one of the sides is above vapor pressure, then conditions are calculated exactly the same as when the valve is closed in the above vapor pressure case, described previously. As before, the valve stays closed until $H_{P\,1,NS} - H_{P\,2,1} > H_{check}$, at which time the valve reopens and conditions revert to the open valve case.

Valve Flowing Out of a System

For the valve flowing out of the system, the downstream pressure head is a defined parameter, H_E. The flowrate through the valve is determined from Eq. (16). Substituting in the known downstream pressure head, combining with Eq. (1) and solving the resulting quadratic equation for flowrate gives:

$$Q_{P\,NS} = -C_V B_1 + \sqrt{C_V^2 B_1^2 + 2C_V\left(C_{P_1} - H_E\right)} \qquad (24)$$

where the NS subscript here refers to the end section of a pipe. $H_{P\,NS}$ is then found from Eq. (1).

When the pressure drops to the vapor pressure, then $H_{P\,NS}$ is determined from Eq. (5), and the flowrate from Eq. (24):

$$Q_{P\,NS} = \frac{Q_o\,\tau}{\sqrt{\Delta H_o}}\sqrt{H_{P\,NS} - H_E}$$
$$= \sqrt{2C_V\left(H_{P\,NS} - H_E\right)}$$

$Q_{PU\,1,NS}$ is then found from Eq. (6), and the vapor cavity size is determined from Eq. (21). If $H_{P\,NS} < H_E$, then the downsteam ambient gas will flow back into the system and a new model would be required that is beyond the scope of this method. Thus, care should be taken that $H_{P\,NS}$ is always greater than H_E.

Dead-end Pipe

The conditions at the end of a dead-end pipe become

$$Q_{P\,NS} = 0$$

and therefore from Eq. (1)

$$H_{P\,NS} = C_P$$

When the pipe end drops to vapor pressure, then the head, $H_{P\,NS}$, is known from Eq. (5) and

$$Q_{P\,NS} = 0$$

$$Q_{PU\,NS} = \frac{(C_P - H_{P\,NS})}{B}$$

The vapor cavity size is then

$$V_{CAV,P\,NS} = V_{CAV\,NS} + (-Q_{PU\,NS} - Q_{U\,NS})\,\Delta t/2$$

Specified Flowrate at System Boundary

A specified flowrate boundary condition results in a known flowrate for all times. The head is then determined from Eq. (2) if the flow is entering the system or from Eq. (1) if the flow is exiting the system. When vapor pressure is reached, then the head, $H_{P\,1,1}$, is found from Eq. (5) and for flow entering the system

$$Q_{PU\,1,1} = Q(t)_{specified}$$

$$Q_{P\,1,1} = \frac{(H_{P\,1,1} - C_{M_1})}{B_1}$$

The vapor cavity size is

$$V_{CAV,P\,1,1} = V_{CAV\,1,1} + (Q_{P\,1,1} + Q_{1,1} - Q_{PU\,1,1} - Q_{U\,1,1})\,\Delta t/2$$

For flow exiting the system

$$Q_{P\,NS} = Q(t)_{specified}$$

$$Q_{PU\,NS} = \frac{(C_P - H_{P\,NS})}{B}$$

and the vapor cavity size is

$$V_{CAV,P\,NS} = V_{CAV\,NS} + (Q_{P\,NS} + Q_{NS} - Q_{PU\,NS} - Q_{U\,NS})\,\Delta t/2$$

Reservoir Boundary

A reservoir boundary models a reservoir connected to a pipe at the inlet or outlet of a system. A reservoir provides a specified pressure head at the end of a pipe. With the head specified, the flowrate at the reservoir is calculated from Eqs. (1, 2).

Because the reservoir defines the pressure head at the reservoir, it is inconsistent for a reservoir to define a pressure that is below vapor pressure. Therefore, vapor pressure can never be reached at the reservoir interface, and Q_U flowrates always equal Q flowrates. However, the section just downstream of an inlet reservoir may reach vapor pressure, thus requiring the use of Eq. (8) in the solution of Eq. (2) for flowrate.

Short Line with Lumped Inertia and Friction

A short pipe in a system requires a short time step, and thus more computation time. This can be avoided by modeling the short pipe segment as a lumped inertia element. Inertia and friction effects are accounted for in the short pipe, but the liquid compressibility and the elasticity of the pipe are ignored. From Figure 4, a force balance on the fluid in Section 2 can be written:

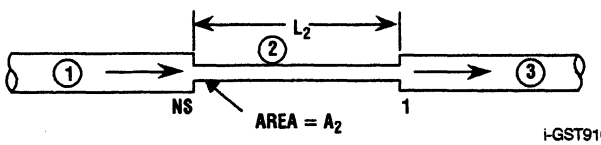

Figure 4. Schematic for short pipe with lumped inertia.

$$F_1 - F_3 - F_f = \varrho\, A_2\, L_2 \frac{dv}{dt} \tag{25}$$

where F_1 and F_3 are the pressure forces acting on the fluid, and F_f is the friction force. By substituting an expression for the friction force, Eq. (25) can also be written

$$\varrho g A_2 \left[\frac{H_{P\,1,NS} + H_{1,NS}}{2} - \frac{H_{P\,3,1} + H_{3,1}}{2} + \frac{f_2 L_2 Q_2 |\,Q_2\,|}{2 g D_2 A_2^2} \right] = \frac{\varrho L_2}{\Delta t}(Q_{P2} - Q_2)$$

This can be simplified to

$$H_{P\,1,NS} - H_{P\,3,1} = C_1 + C_2 Q_{P2} \tag{26}$$

$$C_1 = H_{3,1} - H_{1,NS} + (C_3 - C_2)\,Q_2 \tag{27}$$

$$C_2 = 2L_2/(g A_2\,\Delta t) \tag{28}$$

$$C_3 = f_2 L_2/(g D_2 A_2^2)\,|\,Q_2\,| \tag{29}$$

By mass conservation

$$Q_{P\,1,NS} = Q_{P3,1} = Q_{P2}$$

By combining Eq. (26) with Eqs. (1) and (2), the flowrate through the pipe section can be obtained

$$Q_{P2} = \frac{C_{P_1} - C_1 - C_{M_3}}{B_1 + B_3 + C_2}$$

Once Q_{P2} is calculated, $H_{P\,1,NS}$ and $H_{P\,3,1}$ are found from Eqs. (1) and (2).

Vapor can form at the upstream side of the short pipe, at the downstream side, or both. However, because the pipe fluid is incompressible, no vapor is allowed to form in the short pipe itself. When vapor forms at the downstream side of the pipe, then $H_{P\,3,1}$ is found from Eq. (5), and

$$Q_{P\,3,1} = \frac{(H_{P\,3,1} - C_{M_3})}{B_3}$$

$$Q_{PU\,1,NS} = Q_{P\,1,NS} = Q_{P2} = Q_{PU\,3,1} \neq Q_{P\,3,1}$$

The flowrate, Q_{P2}, is found by combining Eq. (26) with Eq. (1):

$$Q_{P2} = \frac{C_{P_1} - C_1 - H_{P\,3,1}}{B_1 + C_2}$$

Having solved for the flowrate, $H_{P\,1,NS}$ is found from Eq. (1). The vapor cavity size is

$$V_{CAV,P\,3,1} = V_{CAV\,3,1} + (Q_{P\,3,1} + Q_{3,1} - Q_{PU\,3,1} - Q_{U\,3,1})\,\Delta t/2 \tag{30}$$

$$V_{CAV,P\,1,NS} = 0$$

When vapor forms at the upstream side, then the appropriate expression for flow through the pipe is

$$Q_{P2} = \frac{H_{P\,1,1} - C_1 - C_{M_3}}{B_3 + C_2}$$

The vapor cavity size is found from Eq. (21). When vapor forms on both sides of the pipe, then $H_{P\,1,NS}$ and $H_{P\,3,1}$ are found from Eq. (5) and

$$Q_{P\,1,NS} = Q_{P2} = Q_{PU\,3,1}$$

and $Q_{PU\,1,NS}$ and $Q_{P\,3,1}$ are found from Eqs. (6) and (7). Flow is still possible through the short pipe because of inertia from the previous time step. From Eq. (26)

$$H_{P\,1,NS} - H_{P\,3,1} = C_1 + C_2 Q_{P2} = 0 \tag{31}$$

However, a better approximation for C_1 in this case is

$$C_1' = H_{3,1} - H_{1,NS} + C_3 Q_{P2} - C_2 Q_2$$

Substituting C_1' for C_1 in Eq. (31) and solving for Q_{P2} yields

$$Q_{P2} = \frac{H_{1,NS} - H_{3,1} + C_2 Q_2}{C_2 + C_3}$$

The vapor cavity sizes are found from Eqs. (21) and (30).

DISCUSSION

The application of the VCM method to a multi-pipe system suffers from the same limitations as the single-pipe system described by Wylie and Streeter (1983) and Simpson and Wylie (1985). One such limitation is the occurrence of nonphysical pressure spikes in the pressure predictions when distributed vapor cavities form and collapse in a system. In addition, the timing of physical pressure spikes are not always accurately predicted by the model. The advantage of the VCM method is that it is relatively simple when compared to other approaches described by Kamemura, et al. (1988), Baltzer (1967), and Wylie (1984b), and it works with the method of specified time intervals. When used with an understanding of its limitations, the VCM method can be used effectively in many applications.

Comparisons of the VCM method to experimental data in single-pipe systems are made in Wylie and Streeter (1983). Unfortunately, published experimental data of vaporous cavitation in more complicated piping systems are difficult to find. A recent publication by Kamemura, et al. (1988) presents experimental results for the water piping system shown in Figure 5 experiencing an instantaneous valve closure. Three connecting elements are used to model this system: specified flowrate, branch connector (to model the pipe bends), and a reservoir boundary. Figure 6 shows the transient pressures predicted by the multi-pipe VCM method, and compares these predictions with some of the experimental results presented by Kamemura, et al. (1988). Reasonable agreement is obtained, especially on the magnitudes of the pressure peaks. However, the nonphysical spikes inherent in the VCM method are evident, and the timing of some measured pressure spikes are not accurately predicted by the model.

The predicted velocities are compared to the measured velocities in Figure 7. Again, reasonable agreement is obtained. It can be seen that the major features of the flow are predicted by the model. It is interesting to note that although the VCM method assumes small vapor cavity size, the largest predicted vapor cavity at Figure 5 Location 1 is 16% of the computing section volume, and at Location 2 it is 46% of the volume.

CONCLUSIONS

The Vaporous Cavitation Model can be applied to a number of fluid system connecting elements often found in multi-pipe systems. The same limitations that have been identified for single-pipe applications also affect models of multi-pipe systems. However, reasonable agreement can be demonstrated with available data, even though some cavities grow much larger than considered permissible. Peak pressure predictions are shown to agree well with the data, and the major features of the flow are predicted by the model. Additional experiments for complicated fluid systems with vaporous cavitation are required to explicitly verify the models developed in this paper. However, the basic approach of the VCM method is well understood, and the consistent application of the VCM method to multi-pipe fluid elements is a relatively straightforward extension of the method.

REFERENCES

Baltzer, R. A., 1967, "Column Separation Accompanying Liquid Transients," *Journal of Basic Engineering*, Vol. 89, pp. 837–846.

Kamemura, T., Jyowo, K., Hata, T., Hayashi, H., Yoshikai, T., and Kondo, M., 1988, "Fluid Transients in Pipeline," *Nippon Kokan Technical Report Overseas*, No. 52, pp. 42–49.

Simpson, A. R. and Wylie, E. B., 1985, "Problems Encountered in Modeling Vapor Column Separation," *Proceedings of 1985 ASME Winter Meeting*, ASME New York, pp. 103–107.

Streeter, V. L., 1972, "Unsteady Flow Calculations by Numerical Methods," *Journal of Basic Engineering*, Vol. 94, pp. 457–466.

Wylie, E. B., and Streeter, V. L., 1983, *Fluid Transients*, corrected ed., FEB Press, Ann Arbor, MI.

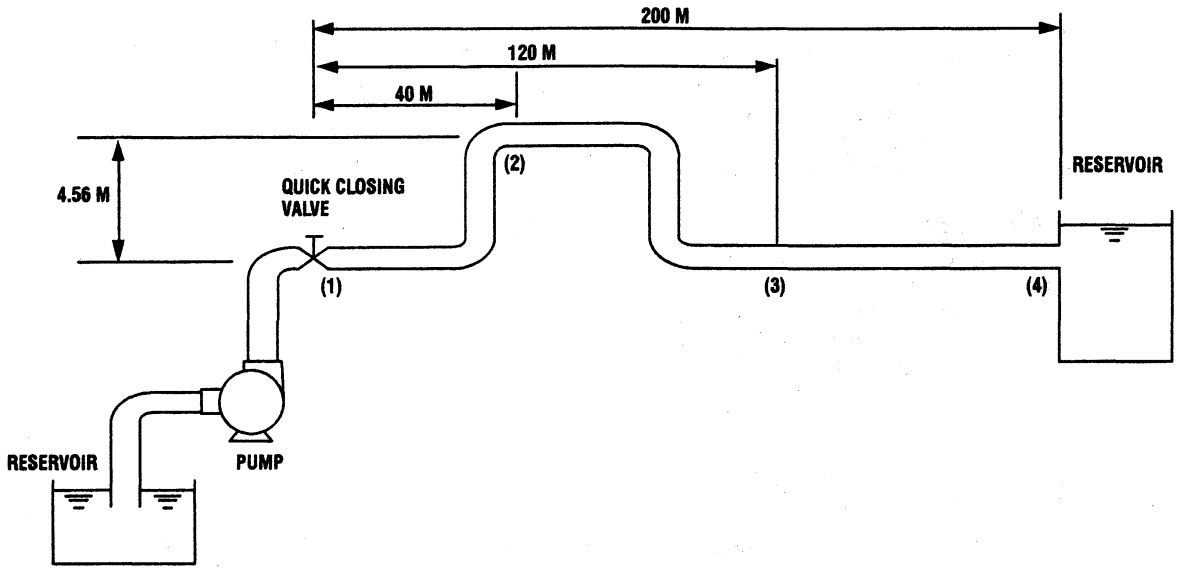

Figure 5. Experimental setup in Kamemura, et al. (1988) for measuring waterhammer data during liquid column separation. Numbers in parentheses refer to measurement locations.

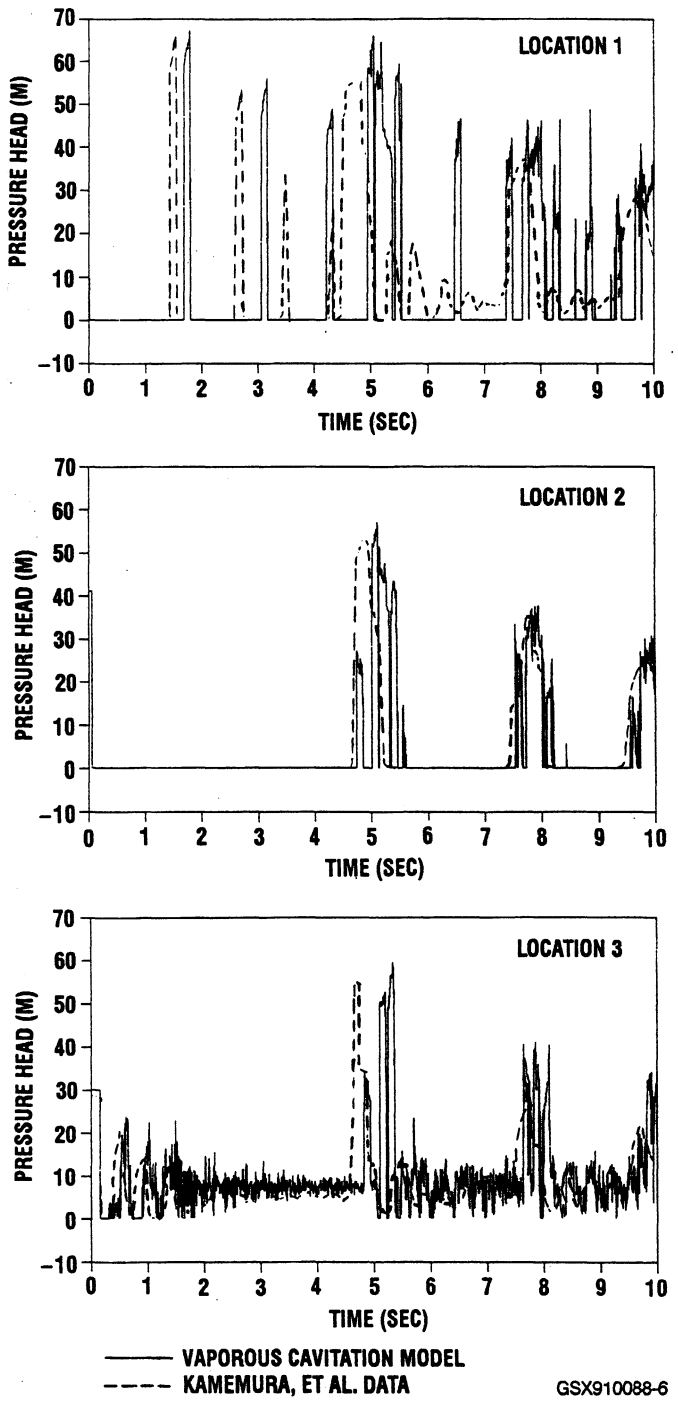

Figure 6. Vaporous Cavitation Model pressure predictions compared to Kamemura et al. (1988) experimental results for Figure 5 configuration.

Wylie, E. B., 1984a, "Fundamental Equations of Waterhammer," *Journal of Hydraulic Engineering*, Vol. 110, pp. 539–542.

Wylie, E. B., 1984b, "Simulation of Vaporous and Gaseous Cavitation," *Journal of Fluids Engineering*, Vol. 106, pp. 307–311.

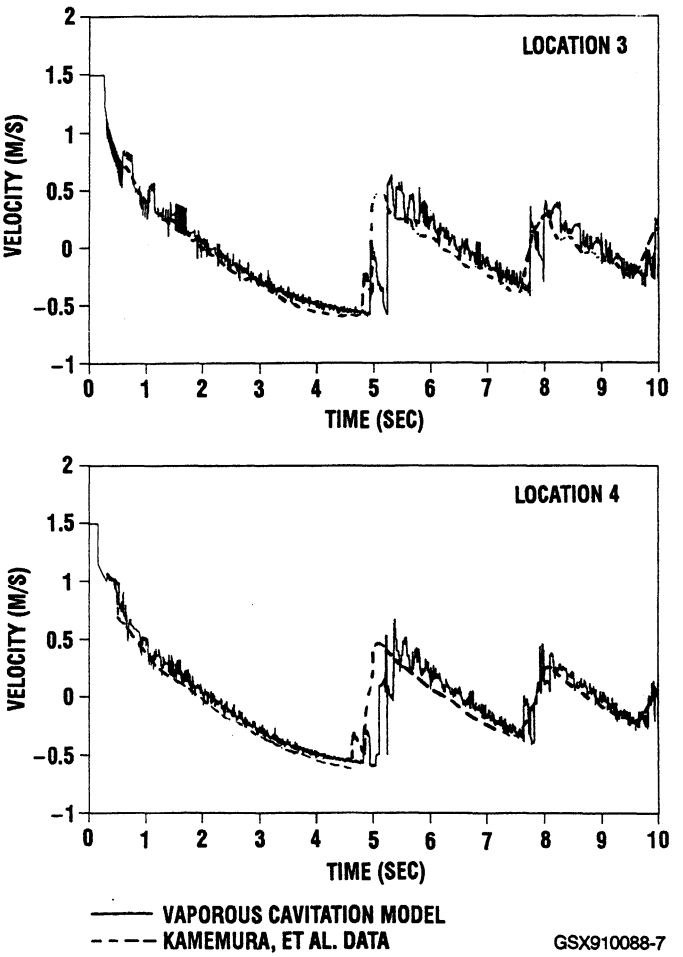

Figure 7. Vaporous Cavitation Model flowrate predictions compared to Kamemura et al. (1988) experimental results for Figure 5 configuration.